

Revealing the Implicit Noise-based Imprint of Generative Models

Xinghan Li¹, Jingjing Chen^{1*}, Yue Yu¹, Xue Song¹, Haijun Shan², Yu-Gang Jiang¹

¹Shanghai Key Lab of Intell. Info. Processing, School of CS, Fudan University, China

²CEC GienTech Technology Co.,Ltd., Shanghai China

{xinghanli24, yueyu24, xuesong21}@m.fudan.edu.cn,

haijun.shan@gientech.com, {chenjingjing, ygj}@fudan.edu.cn

Abstract

With the rapid advancement of vision generation models, the potential security risks stemming from synthetic visual content have garnered increasing attention, posing significant challenges for AI-generated image detection. Existing methods suffer from inadequate generalization capabilities, resulting in unsatisfactory performance on emerging generative models. To address this issue, this paper presents a novel framework that leverages noise-based model-specific imprint for the detection task. Specifically, we propose a novel noise-based imprint simulator to capture intrinsic patterns imprinted in images generated by different models. By aggregating imprints from various generative models, imprints of future models can be extrapolated to expand training data, thereby enhancing generalization and robustness. Furthermore, we design a new pipeline that pioneers the use of noise patterns, derived from a noise-based imprint extractor, alongside other visual features for AI-generated image detection, resulting in a significant improvement in performance. Our approach achieves state-of-the-art performance across three public benchmarks including GenImage, Synthbuster and Chameleon.

1. Introduction

The advancement of deep generative models has led to a remarkable improvement in synthesized image quality. Notably, recent methods [5, 18, 25, 29, 41] have demonstrated impressive capabilities in generating photorealistic images that are nearly indistinguishable from real ones. While these developments have achieved both academic and commercial success, they have also given rise to serious risks, such as misinformation propagation [37] and identity fraud [4]. Therefore, it is crucial to develop robust and generalizable detectors to distinguish AI-generated images.

Existing detection approaches [13, 24, 33, 34, 36] have

*Corresponding author.

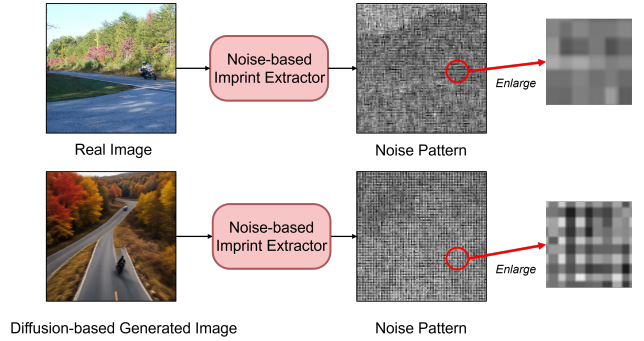


Figure 1. **The different noise patterns between real image and AI-generated image.** The first row shows the real image, while the second row displays the image generated by a diffusion-based model (with the prompt: “A motorcyclist rides on a winding road surrounded by trees with autumn colors”). Using the Noise-based Imprint Extractor we introduced, we extract the noise pattern.

demonstrated effectiveness when applied to known generative models. For example, works [24, 38] utilizing large pre-trained vision-language models like CLIP [26] to capture semantic features show promising results. However, these methods exhibit significant performance deterioration when challenged with unseen synthesis technologies. This limitation primarily stems from inherent biases in detector’s training data that favor existing generative models, causing detectors to identify characteristics especially for a single model rather than universal patterns. Although some methods [11, 27] attempt to align data by injecting forensic artifacts into real images for training, the result remains heavily dependent on the architectures used, hindering their generalization to unseen models. Therefore, the critical challenge lies in developing detection methodologies that overcome these data-induced biases to achieve robust performance across diverse generative paradigms, particularly as new techniques continue to emerge.

To address the issues mentioned above, we propose a novel solution. Analogous to how camera sensor and optical

process [19, 39] imprinting unique physical noise patterns on real images, we posit that generative models [29, 32] inevitably introduce distinct noise patterns during the synthesis process, which differ from those in real images. As shown in the Figure 1, the noise patterns of real images and AI-generated images are inconsistent. We refer to it as “**Noise-based Imprint**”. These patterns are independent of the image semantic content and are considered an imprint left by the generative model during synthesis, serving as reliable cues for detection. Therefore, to enhance the generalization capability of the detector, we shift the focus from learning task-specific features to modeling fundamental noise discrepancies inherent in the synthesis process itself.

To this end, we propose **NIRNet** (**Noise-based Imprint Revealing Network**), a novel and generalizable framework that leverages noise-based imprint for detecting AI-generated images, which consists of two consecutive stages — a simulation stage and a training stage. In the simulation stage, we firstly introduce a novel noise-based imprint simulator. Through this module, we perform reconstruction of real images using various generative models, modeling the differences before and after reconstruction as noise-based imprints, which represent artificial traces introduced by the synthesis process. Subsequently, we sample from the modeled mixed distribution, which is obtained by mixing the distributions from different models. Through this approach, real images are transformed to incorporate noise-based model-specific imprint and subsequently used as negative samples in the training process, reducing data-induced biases to enhance generalization capabilities and robustness. In the training stage, we design a new pipeline incorporating a Noise-based Imprint Extractor to extract imprints in input images. Furthermore, we utilize a discriminator with hybrid features, which integrates noise feature maps from the Noise-base Imprint Extractor along with frequency and semantic features, to achieve precise differentiation between real and fake images, even for artificial images generated by unseen models.

Overall, our contribution can be summarized as follows:

- We propose NIRNet (Noise-based Imprint Revealing Network), a novel framework including a noise-based imprint simulator that captures intrinsic synthesis process patterns across diverse models, enabling extrapolation for training data, fundamentally shifting focus from singular artifacts to universal noise patterns.
- We pioneer the integration of noise-based imprint with frequency and semantic features in our detection pipeline.
- Our extensive experimental evaluation demonstrates that NIRNet achieves state-of-the-art performance across three public benchmarks including GenImage [42], Synthbuster [3] and Chameleon [38], particularly excelling in cross-model generalization scenarios.

2. Related Work

With the rapid development of generative models, distinguishing between real and AI-generated images has become increasingly challenging. As a result, the demand for detecting AI-generated images is growing.

Detection via Inherent Artifact Analysis. Early approaches focused on identifying differences in image cues, such as reflections [23], color [20], co-occurrence [22], and saturation [21]. However, these methods often struggle with generalization as generative models evolve. To address this limitation, CNNSpot [35] proposes training a convolutional neural network as a binary classifier to directly differentiate between real and AI-generated images. It is trained exclusively on ProGAN [14] but can effectively generalize to other unseen GAN architectures through careful pre-processing, post-processing, and data augmentation. Frequency-based approaches [9, 16, 38, 40] identify significant artifacts in the frequency domain of synthesized images, which are caused by the up-sampling operations in the generation process. Gradient-based methods [33], on the other hand, convert images into gradient-based representations, utilizing gradients as a generalized form of artifacts produced by generative models. Semantic-based methods [7, 24] show that linear probing of a pre-trained, frozen CLIP image encoder can effectively detect fake images generated by a wide range of models. Additionally, reconstruction-based method [36] employ DDIM inversion to reconstruct images and then train a classifier to detect differences. Another work [28] extends this approach to Latent Diffusion Models, using VAE-based reconstructions and LPIPS distance for detection.

Detection via Simulated Artifact Injection. Apart from the aforementioned methods, artifact injection-based methods are more closely related to ours. Prior research has explored creating simulated fake images by injecting generative process traces into real images. For GAN-generated image detection, FingerprintNet [12] reconstructs real images and embeds synthesized fingerprints that simulate artifacts produced during up-sampling processes in the frequency domain. In the context of diffusion-generated image detection, DRCT [6] employed DDIM [31] inversion to reconstruct both authentic and synthetic images, incorporating both types into contrastive learning frameworks during training. Study [27] utilized the VAE [15] autoencoder from LDM to reconstruct real images without engaging the diffusion model’s denoising procedure, thereby introducing artifacts inherent to the VAE. The approach in [11] integrated autoencoder techniques with diffusion steps, leveraging the inpainting diffusion model of Stable Diffusion 2.1 [30] to generate self-synthesized images. In contrast to these methodologies, our approach models artifacts across multiple generative models and injects them into training data by sampling from the modeled distribution. This strat-

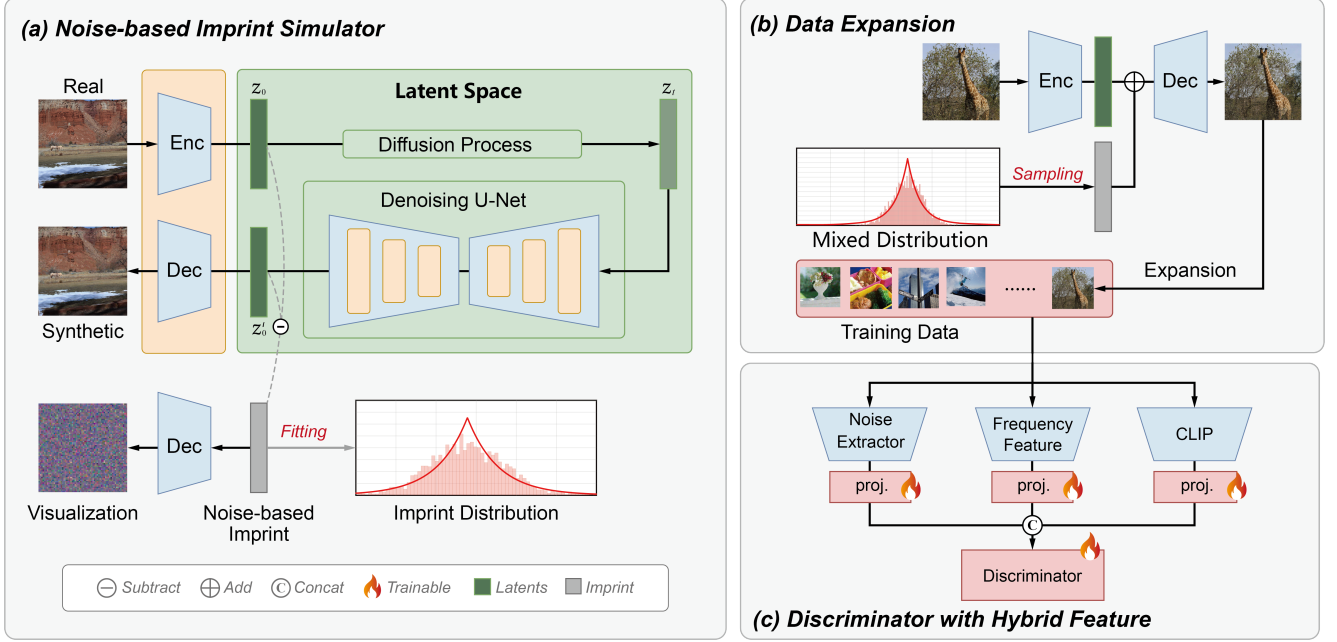


Figure 2. **Overall framework of the proposed NIRNet.** Our NIRNet consists of two stages: a simulation stage and a training stage. In the simulation stage (a) and (b), we introduce a Noise-based Imprint Simulator to model the noise-based imprint of the generative model. This process leverages the differences computed after reconstruction, which are learned and fitted to a Laplacian distribution. Subsequently, samples are drawn from a mixed distribution derived from multiple models to transform real images into images embedded with imprint, thereby expanding the training dataset. In the training stage (c), end-to-end training is performed on the expanded dataset. A noise-based imprint extractor, utilized to capture the intrinsic noise pattern of images, is introduced. In conjunction with frequency and semantic features, our framework functions in a hybrid feature manner to detect AI-generated images.

egy enhances diversity in the simulated out-of-distribution noise patterns, largely improving the generalization capability of our model.

3. Methodology

As shown in Figure 2, our proposed approach consists of two consecutive stages. In the first stage, we focus on modeling the noise imprint embedded in AI-generated images through our Noise-based Imprint Simulator. This simulator extracts model-specific imprints by analyzing reconstruction differences, enabling the expansion of the training dataset by transforming real images with simulated imprint. In the second stage, we perform end-to-end detection. A Noise-based Imprint Extractor is introduced to capture intrinsic noise patterns. These patterns are integrated with frequency and semantic features in a hybrid manner. In the following sections, we will detail the key components and design principles within each stage of our framework.

3.1. Preliminary

Diffusion-based models currently represent the forefront of image generation, producing images that are virtually indistinguishable from real ones. Therefore, we have designed a method for learning the noise-based imprint of these mod-

els. First, we briefly introduce the diffusion process. Diffusion models [31, 32] have demonstrated exceptional performance in image generation. These models operate through forward and reverse diffusion processes. The forward process gradually adds noise to a latent representation \mathbf{z}_0 over T timesteps:

$$q(\mathbf{z}_t|\mathbf{z}_{t-1}) = \mathcal{N}(\mathbf{z}_t; \sqrt{1 - \beta_t} \mathbf{z}_{t-1}, \beta_t \mathbf{I}), \quad (1)$$

where $\beta_t \in (0, 1)$ is the noise variance at step t . The reverse process reconstructs the original representation by denoising:

$$p_\theta(\mathbf{z}_{t-1}|\mathbf{z}_t) = \mathcal{N}(\mathbf{z}_{t-1}; \mu_\theta(\mathbf{z}_t, t), \Sigma_\theta(\mathbf{z}_t, t)), \quad (2)$$

where μ_θ and Σ_θ are learnable parameters. Starting from a noisy representation \mathbf{z}_T , the output \mathbf{z}'_0 is obtained through:

$$\mathbf{z}'_0 = \mathcal{D}(\mathbf{z}_T, \theta), \quad (3)$$

where $\mathcal{D}(\cdot, \theta)$ denotes the denoising process with parameters θ controlling inference steps and denoising strength.

3.2. Simulator and Data Expansion

Noise-based Imprint Simulator. We propose a module designed to extract noise patterns from generated images,

which serve as an imprint of the generative model. As mentioned above, an image can contain various noise patterns that may reveal its source. We hypothesize that AI-generated images similarly exhibit distinctive noise patterns and this noise could be regarded as an imprint left by the generative model during synthesis. By identifying this imprint, models can generalize better to detect images.

Diffusion-based models primarily operate within latent space, where they introduce model-specific inherent noise during the image generation process. Especially, we model this noise-based imprint as a distribution derived from images generated by a specific model. To learn this imprint, we reconstruct an image using the generative model and measure the differences before and after reconstruction. Specifically, for a given real image I , we first encode it into latent space using a VAE [15] to obtain \mathbf{z}_0 . We then add noise to \mathbf{z}_0 and denoise it using a pre-trained model to obtain \mathbf{z}'_0 . The difference between \mathbf{z}_0 and \mathbf{z}'_0 is considered as the noise-based imprint added by the model, as expressed in the following equation:

$$\Delta \mathbf{z} = \mathbf{z}'_0 - \mathbf{z}_0. \quad (4)$$

We model the above difference using a Laplace distribution. This is motivated by the distribution’s robust capability, capturing sparse, heavy-tailed perturbations that commonly arise during iterative generation processes, particularly in the multi-step denoising characteristic of diffusion models. Furthermore, the Laplace distribution’s distinctive peak and exponentially decaying tails make it especially well-suited to accommodate substantial fluctuations. For a set of n real images, we obtain the corresponding reconstruction differences, denoted as $\mathbf{X} \in \mathbb{R}^{n \times C \times H \times W}$, where C is the number of channels, and H and W denote the height and width, respectively. By computing the mean and standard deviation along the dimension of the number n of differences, we derive the mean $\boldsymbol{\mu} \in \mathbb{R}^{C \times H \times W}$ and the standard deviation $\boldsymbol{\sigma} \in \mathbb{R}^{C \times H \times W}$, where

$$\boldsymbol{\mu}_{c,h,w} = \frac{1}{n} \sum_{i=1}^n \mathbf{X}_{i,c,h,w}, \quad (5)$$

$$\boldsymbol{\sigma}_{c,h,w} = \sqrt{\frac{1}{n} \sum_{i=1}^n (\mathbf{X}_{i,c,h,w} - \boldsymbol{\mu}_{c,h,w})^2}. \quad (6)$$

The scale parameter is defined as $\mathbf{b} = \frac{\boldsymbol{\sigma}}{\sqrt{2}}$, so that the reconstruction differences can be modeled as

$$\mathbf{X} \sim \text{Laplace}(\boldsymbol{\mu}, \mathbf{b}). \quad (7)$$

Expansion of Training Data. After extracting noise patterns from various models, our objective is to extrapolate these patterns to predict the noise-based imprint of unseen or future models. Our analysis as illustrated in the

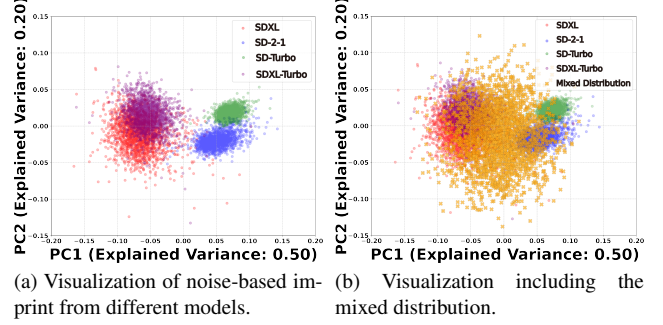


Figure 3. PCA visualizations showing the distributions of noise-based imprint: (a) from different models, and (b) with the addition of a mixed distribution.

Figure 3a, reveals several key characteristics: (1) the distributions of noise-based imprint vary significantly across models rather than adhering to a single, uniform distribution; (2) models with similar architectures exhibit comparatively minor differences in their noise pattern distributions; and (3) despite these differences, the noise patterns do not diverge drastically, as evidenced by overlapping samples across models. Based on these observations, we propose that a mixed distribution, obtained by mixing the distributions from different models, can effectively encompass the full range of noise patterns, as shown in Figure 3b. We further hypothesize that this mixed distribution will simulate the noise patterns of both unseen and future models. Building on this insight, we introduce a data expansion method to extrapolate images generated by unseen models. Specifically, for a given image x , we first encode it to obtain its latent representation \mathbf{z}_0 . Next, an imprint $\Delta \mathbf{z}^*$ is sampled from the mixed distribution X' of differences derived from multiple models. This imprint is then added to \mathbf{z}_0 to yield an adjusted latent representation:

$$\mathbf{z}_0^* = \mathbf{z}_0 + \Delta \mathbf{z}^*. \quad (8)$$

Subsequently, \mathbf{z}_0^* is decoded to produce an image x^* , which corresponds to an image generated by some unseen models. Through this approach, real images are transformed to incorporate noise-based model-specific imprint and subsequently used to replace a portion of the negative samples in the training process. Consequently, the model is exposed to a broader range of generated images beyond those from known models, preventing its detection patterns from collapsing into a few fixed modes and thereby enhancing its generalization capability when confronted with unseen or future models.

3.3. Pipeline

We propose a novel framework that, for the first time, enables the detection of AI-generated images by extracting model-specific noise patterns. As shown in the Figure 2,

this framework consists of three feature extraction modules and a discriminator in a mixture of experts manner, which are trained end-to-end on an expanded dataset.

Noise-based Imprint Extractor. We pioneer the use of image noise patterns for distinguishing AI-generated images. Real images retain distinct imprint from their capture and storage processes, whereas AI-generated content lacks the sensor noise characteristics inherent to original cameras. As a result, noise extractors detect different noise patterns when processing real versus generated images. To leverage these different patterns, we utilize a pre-trained noise extractor [10], initially designed for forgery detection and localization, to extract noise-based imprint features from input images. This extractor yields a single-channel noise-sensitive feature map, F_n . To prepare this map for inputting into the discriminator, we apply a trainable layer for further transformation.

Discriminator with Hybrid Features. For the discriminator, we utilize the feature of noise-based imprint alongside two additional feature types, high-frequency and semantic features, to achieve comprehensive discrimination. Specifically, a Frequency Extractor is employed to derive high-frequency features F_f . Given that generative models frequently produce excessive smoothness or anti-aliasing effects [38], these high-frequency features effectively capture such artifacts. In parallel, semantic features are extracted to capture inherent image semantics. In the context of low-quality AI-generated image, these semantic features tend to exhibit out-of-distribution characteristics, thereby facilitating efficient detection. Following extraction, semantic features are refined through average pooling. Ultimately, the three distinct features are concatenated and fed into an MLP discriminator, with the whole model being trained end-to-end on the expanded dataset.

4. Experiment

4.1. Experimental Setup

Dataset. We evaluate our method on three benchmark datasets, including **GenImage** [42], **Synthbuster** [3] and **Chameleon** [38]. GenImage is a large-scale benchmark dataset for AI-generated image detection that covers eight popular generation models, consisting of both diffusion models (e.g., Midjourney, Stable Diffusion) and GAN models (e.g., BigGAN). In total, it contains 2,681,167 images, including 1350000 generated images and 1331167 real images. GenImage provides both training set and testing set. For each generation method, 6,000 generated images and 6,000 real images are used for testing. Unlike the GenImage dataset, both the Synthbuster and Chameleon datasets contain only a testing set. The Synthbuster dataset is specifically designed to evaluate methods for detecting images generated by state-of-the-art diffusion models, in-

cluding Stable Diffusion, Midjourney, GLIDE, Firefly and DALL-E. The corresponding real images, 1000 real images for each subset, are sourced from the RAISE dataset [8]. The Chameleon dataset is a more challenging benchmark dataset, containing 26,000 images that covers human, animal, object, and scene categories. It is worth mentioning that, unlike the Synthbuster dataset, the AI-generated images in the Chameleon dataset are entirely produced by unknown generation methods. Notably, all AI-generated images have passed human perception tests, making it a more challenging benchmark for detectors.

In addition to testing on three publicly available datasets, we collected a small test dataset for further evaluation. This dataset focuses on distinguishing images generated by the latest generation methods, FLUX.1-dev [1] and Stable Diffusion 3.5 [2], which are not included in the previous three benchmark datasets. For each generation method, we collected 2,000 images. Additionally, similar to Synthbuster, we used 4,000 real images from RAISE-4k for evaluation. In total, our dataset comprises 8,000 images, and we refer to it as **Gen-8K**.

Implementation details. For Noise-based Imprint Simulator, we employ the VAE from the LDM [29] model for latent encoding and decoding. To model noise distribution, 2,000 high-quality images from the RAISE dataset are used. Pre-trained diffusion models, including SD 2.1, SD-Turbo, SDXL, SDXL-Turbo, are used to reconstruct images. These models are empirically configured with 400 inference steps, a strength of 0.1, and a guidance scale of 0.0 as parameters in the image-to-image pipeline. Noise from the modeled distribution, with intensity randomly sampled from 0.15 to 0.5, is injected into latent representations of 2% of real training images, with five independent noise samples synthesized per image, replacing the original fake images in the training dataset. We use the pre-trained weights from Noiseprint++ [10] to initialize our Noise-base Imprint Extractor.

Since our objective is to evaluate the model’s generalization ability, we do not use the entire training set from GenImage. Instead, we following [38], and train the detection model solely on images generated by Stable Diffusion V1.4. We then assess its performance on testing sets that include a diverse range of generation methods. Following previous work [35], data augmentation strategies, including random JPEG compression with quality factor $QF \sim \text{Uniform}(30, 100)$ and random Gaussian blur with $\sigma \sim \text{Uniform}(0.1, 3.0)$, are applied. In training, AdamW is chosen as the optimizer, and the learning rate is set as 1×10^{-4} . The experiments are conducted on 8 NVIDIA RTX 4090 GPUs with a batch size set as 32. Our model is trained for 10 epochs.

Evaluation Metric. Following previous work [35, 38], we use classification accuracy (Acc) and average precision

Method	Midjourney	SD v1.4	SD v1.5	ADM	GLIDE	Wukong	VQDM	BigGAN	Avg.
CNNSpot [35]	54.98	86.83	86.90	48.85	48.48	86.12	52.78	49.28	64.28
FreDect [9]	56.33	93.56	93.43	48.46	49.07	92.20	51.18	48.01	66.53
Fusing [13]	70.15	97.95	97.84	54.33	58.37	97.90	50.35	49.18	72.01
LNP [16]	55.78	97.04	96.51	48.36	48.95	94.69	51.25	48.05	67.58
Lgrad [33]	65.88	99.62	99.38	52.63	52.24	97.98	52.68	49.80	71.27
DIRE [36]	66.48	99.63	99.43	51.38	53.78	98.87	51.70	49.73	71.38
UnivFD [24]	62.13	99.74	99.65	50.38	56.47	98.52	92.83	50.02	76.22
NPR [34]	66.38	98.91	98.84	55.60	67.68	97.58	60.25	<u>54.20</u>	74.93
AIDE [38]	<u>83.08</u>	99.88	99.83	<u>73.33</u>	<u>94.17</u>	99.84	<u>93.08</u>	52.24	<u>86.93</u>
<i>NIRNet (Ours)</i>	89.37	<u>99.76</u>	<u>99.68</u>	89.90	97.71	<u>99.33</u>	97.69	63.88	92.17

Table 1. **Comparison on the GenImage dataset [42]**. Accuracy (%) of different detectors (rows) in detecting real and fake images from different generators (columns). These methods are trained on real images from ImageNet and fake images generated by SD v1.4 and evaluated over eight generators. The best result and the second-best result are marked in **bold** and underline, respectively.

Method	SD v2	SD v1.3	GLIDE	Firefly	DALLE3	DALLE2	Midjourney	SD v1.4	SDXL	Avg.
CNNSpot [35]	58.02	66.55	34.87	44.85	44.23	40.89	40.03	67.23	43.83	48.94
FreDect [9]	58.00	82.40	49.85	49.50	50.90	50.60	50.95	82.75	54.15	58.78
Fusing [13]	58.44	<u>99.00</u>	57.89	50.25	74.28	52.10	59.24	<u>99.15</u>	61.53	67.98
LNP [16]	<u>64.35</u>	86.60	49.25	54.85	56.50	52.55	50.55	85.40	55.56	61.73
Lgrad [33]	59.79	98.05	54.04	<u>50.80</u>	<u>60.64</u>	51.29	54.69	97.60	61.04	65.32
DIRE [36]	60.84	98.25	53.25	50.49	51.19	51.40	53.45	98.20	60.04	64.12
UnivFD [24]	56.20	99.70	62.15	50.65	54.90	<u>52.70</u>	58.30	99.45	<u>62.55</u>	66.28
NPR [34]	51.10	95.35	62.23	49.30	51.39	51.35	50.90	95.35	54.04	62.33
AIDE [38]	64.70	92.90	<u>78.60</u>	41.15	55.95	47.20	<u>76.05</u>	93.90	62.10	<u>68.06</u>
<i>NIRNet (Ours)</i>	75.75	84.35	79.40	34.85	57.40	64.90	77.35	84.35	78.75	70.79

Table 2. **Comparison on the Synthbuster dataset [3]**. Accuracy (%) of different detectors (rows) in detecting real and fake images from different generators (columns). The best result and the second-best result are marked in **bold** and underline, respectively.

(AP) as evaluation metrics in our experiments. Unless otherwise specified, all results are averaged across both real and AI-generated images. In the main paper, we primarily report Acc for evaluation and comparison, while AP results are provided in the supplementary materials.

4.2. State-of-the-art Comparison

To ensure a fair comparison, we only consider the methods with publicly available code for evaluation. We compare with 9 methods including CNNSpot [35], FreDect [9], Fusing [13], LNP [16], LGrad [33], DIRE [36], UnivFD [24], NPR [34], and AIDE [38].

- **CNNSpot** [35] enhances the generalization ability of detection models through data augmentation techniques, including JPEG compression and Gaussian blur.
- **FreDect** [9] leverages artifacts in the frequency domain

for fake image detection.

- **Fusing** [13] integrates global spatial information and local patch features to improve classifier performance.
- **LNP** [16] extracts noise patterns from images using a pre-trained denoising network and identifies fake images based on frequency-domain analysis.
- **LGrad** [33] utilizes gradient maps obtained from a pre-trained CNN to capture image fingerprints for detection.
- **DIRE** [36] observes obvious differences in discrepancies between images and their reconstruction by diffusion model and uses this feature as a fingerprint for detection.
- **UnivFD** [24] trains the detector using features extracted by CLIP.
- **NPR** [34] demonstrates that up-sampling operators can cause generalized forgery artifacts beyond frequency-based artifacts.

- **AIDE** [38] presents a mixture-of-expert model that enables discerning AI-generated images based on both low-level pixel statistics and high-level semantics.

Result on the GenImage dataset. Table 1 summarizes the results on GenImage dataset. From the results, we have the following observations. Firstly, for existing methods, when tested on images generated by SD v1.4, SD v1.5, or Wukong, which share the same or a similar architecture as SD v1.4 (the model used to generate the training data)—most detection models achieve an accuracy of around 99%. However, their performance drops significantly when applied to images generated by those with less similarity to the training data, such as ADM, GLIDE, VQDM, and BigGAN. These results highlight the limited generalization ability of existing detection methods. Secondly, among all the methods, our NIRNet achieves the highest performance in terms of mean accuracy, outperforming AIDE—the second-best method by 5.1%. The results demonstrate that our method can significantly improve the generalization ability in generated image detection. The superiority of our method is particularly evident in handling diffusion models with different architectures. On ADM and BigGAN, our methods demonstrate the best generalization ability, it outperforms over 11% than AIDE—the second-best method. Third, since the detection models are trained on SD v1.4, it is not surprising that their performance drops significantly on GAN-generated images. However, as our model includes a module designed to extract noise imprint including camera devices and generative models, it still achieves a detection accuracy of 63.88%.

Result on the Synthbuster dataset. We then evaluate our method on the Synthbuster dataset, and the results are summarized in Table 2. From the results, our NIRNet achieves the best average accuracy, which is 2.8% higher than the second best performances obtained from AIDE. Also, for the majority of generation methods, our approach achieves the highest detection accuracy. It is worth noting that, compared to the results on GenImage, the detection performance on Synthbuster exhibits a significant decline. This is because Synthbuster presents a greater challenge, as it contains more complex scenes than GenImage.

Result on the Chameleon dataset. We further evaluate our NIRNet on the Chameleon dataset in Table 3. Since the generated images come from unknown methods, we report only the overall performance rather than the performance for each individual generation method. Furthermore, since we do not know whether the images are generated by diffusion models or GAN-based models, we also report the performance using ProGAN [35] as the training data. Table 3 summarizes the results. Overall, consistent with the results on the GenImage and Synthbuster datasets, our NIRNet achieves the best performance across different settings. When trained on images generated by SD V1.4, NIRNet at-

tains an average accuracy of 65.41%, outperforming AIDE by 2.8%. These results highlight the superior generalization ability of our method.

Result on our Gen-8K dataset. We report the performance comparison results on Gen-8K in Table 4. Our method demonstrates exceptional cross-architecture generalization capability. Most existing methods achieve around 60% accuracy or lower when detecting images from SD 3.5 and FLUX.1-dev. In contrast, our approach significantly outperforms these baselines, attaining approximately 74% accuracy on SD 3.5 and around 80% on FLUX. This substantial performance gain highlights our method’s ability to capture fundamental artifacts or intrinsic patterns to the generative process, rather than merely overfitting to specific generator architectures.

Method	SD 3.5		FLUX	
	Simp	Qual	Simp	Qual
CNNSpot [35]	58.50	53.35	45.20	41.35
FreDect [9]	57.20	54.30	52.70	49.90
Fusing [13]	60.15	58.55	59.00	57.45
LNP [16]	60.10	58.05	56.90	54.15
Lgrad [33]	56.00	54.90	55.85	54.10
DIRE [36]	58.80	55.95	55.35	54.20
UnivFD [24]	59.60	56.05	59.20	55.80
NPR [34]	60.70	57.90	61.30	59.00
AIDE [38]	56.95	56.35	63.50	62.50
NIRNet (Ours)	74.35	74.60	79.80	81.25

Table 4. **Comparison on our Gen-8K dataset.** Detection accuracy (%) on images generated by SD 3.5 and FLUX.1-dev. Simp and Qual refer to images generated using simple and quality prompts, respectively.

4.3. Ablation Study

To validate the effectiveness of our proposed components and understand their individual contributions to the overall performance, we conducted a series of ablation experiments on the NIRNet framework. Specifically, we evaluated four configurations: (1) a baseline model without our proposed modules, (2) integration of only the Noise-based Imprint Simulator (NIS) for training data expansion, (3) integration of only the Noise-based Imprint Extractor (NIE), and (4) our complete architecture with both modules. Table 5 summarizes the results obtained under different configurations on the dataset GenImage [42].

The baseline model achieved a mean accuracy of 86.19%, demonstrating reasonable performance but with significant room for improvement. Incorporating the data expansion from NIS alone increased accuracy to 89.12%, representing a 2.93% improvement. This confirms our hy-

Training Dataset	CNNSpot [35]	FreDect [9]	Fusing [13]	GramNet [17]	LNP [16]	UnivFD [24]	DIRE [36]	NPR [34]	AIDE [38]	NIRNet (Ours)
ProGAN	56.94	55.62	56.98	58.94	57.11	57.22	58.19	57.29	58.37	59.11
	0.08/99.67	13.72/87.12	0.01/99.79	4.76/99.66	0.09/99.97	3.18/97.83	3.25/99.48	2.20/98.70	5.04/98.46	5.29/99.56
SD V1.4	60.11	56.86	57.07	60.95	55.63	55.62	59.71	58.13	62.60	65.41
	8.86/98.63	1.37/98.57	0.00/99.96	17.65/93.50	0.57/97.01	74.97/41.09	11.86/95.67	2.43/100.00	20.33/94.38	32.95/89.81

Table 3. **Comparison on the Chameleon [38]**. Accuracy (%) of different detectors (rows) in detecting real and fake images of Chameleon. For each training dataset, the first row indicates the **Acc** evaluated on the Chameleon testset, and the second row gives the **Acc** for “**fake image / real image**” for detailed analysis.

pothesis that modeling noise-based imprint through noise injection enhances the model’s ability to identify synthetic artifacts characteristic of AI-generated images. Similarly, integrating only the NIE module yielded an accuracy of 88.81%, a 2.62% improvement over the baseline. This demonstrates the effectiveness of capturing noise patterns for distinguishing between real and AI-generated images. The comparable improvements from both modules individually indicate that they address complementary aspects of the detection task. Most notably, the combination of both modules in our complete NIRNet framework achieved the highest accuracy of 92.17%, representing a substantial 6.0% improvement over the baseline. This synergistic effect (exceeding the sum of individual improvements) suggests that the two modules capture fundamentally different but complementary features—Noise-based Imprint Simulator focuses on generative artifacts, while Noise-based Imprint Extractor emphasizes noise patterns.

Module		Avg. Acc.
NIS	NIE	
✗	✗	86.19
✓	✗	89.12
✗	✓	88.81
✓	✓	92.17

Table 5. **Ablation studies on NIS and NIE modules.**

These results substantiate the validity of our proposed approach and its theoretical foundation. The Noise-based Imprint Simulator, with its Laplace distribution modeling of latent space perturbations, effectively captures the unique noise characteristics introduced during the synthesis process. Concurrently, the Noise-base Imprint Extractor successfully extracts the difference in image noise patterns between real images and AI-generated images. Together, they form a robust detection system that leverages multiple discriminative cues.

4.4. Effectiveness to Perturbations

To evaluate real-world applicability, we tested detection performance under common image perturbations: JPEG

compression (*quality*=95, 90) and Gaussian blur (σ =1.0, 2.0), following [35]. The results are shown in Table 6. Results for additional perturbation settings can be found in the supplementary materials.

NIRNet demonstrates superior effectiveness across all perturbation scenarios. Under JPEG compression with QF=90, NIRNet maintains 78.20% accuracy compared to AIDE’s 72.09%. Similarly, with Gaussian blur (σ =2.0), NIRNet achieves 81.55%, outperforming AIDE’s 78.68%. This stems from two key designs: (1) The Noise-based Imprint Simulator captures diverse synthesis noise patterns, making it less sensitive to minor perturbations affecting high-frequency components; (2) The Noise-based Imprint Extractor focuses on fundamental camera-vs-generative process differences rather than surface-level artifacts that are easily disrupted by post-processing. These results highlight NIRNet’s practical advantage in real-world scenarios where images routinely undergo various post-processing operations.

Method	Original	JPEG Compression		Gaussian Blur	
		QF=95	QF=90	σ =1.0	σ =2.0
CNNSpot [35]	64.28	62.10	61.90	62.62	62.54
FreDect [9]	66.53	65.95	65.78	65.61	65.35
Fusing [13]	72.01	71.43	69.60	71.09	70.75
LNP [16]	67.58	67.69	67.42	67.79	67.80
LGrad [33]	71.27	70.72	70.65	70.74	70.85
DIRE [36]	71.38	70.88	70.63	70.92	70.81
UnivFD [24]	76.22	70.25	70.00	70.82	70.82
NPR [34]	74.93	72.18	72.08	74.07	74.35
AIDE [38]	86.93	72.88	72.09	77.26	78.68
NIRNet (Ours)	92.17	79.81	78.20	83.09	81.55

Table 6. **Effectiveness to JPEG Compression and Gaussian Blur.** The classification accuracy is averaged over 8 test sets in [42] with image perturbations.

5. Conclusion

We propose a framework for detecting AI-generated images by leveraging noise-based imprints. Our method simulates noise imprints to expand the training dataset and extracts noise-based imprints, along with frequency and semantic

features, for accurate detection. This approach enhances generalization to unseen generative models. Experimental results show improved detection performance. Future work will focus on refining noise extraction and boosting efficiency.

References

- [1] Flux.1-dev. <https://huggingface.co/black-forest-labs/FLUX.1-dev>. 5
- [2] Stable diffusion 3.5. <https://github.com/Stability-AI/sd3.5>. 5
- [3] Quentin Bammey. Synthbuster: Towards detection of diffusion model generated images. *IEEE Open Journal of Signal Processing*, 5:1–9, 2023. 2, 5, 6
- [4] Clark Barrett, Brad Boyd, Elie Bursztein, Nicholas Carlini, Brad Chen, Jihye Choi, Amrita Roy Chowdhury, Mihai Christodorescu, Anupam Datta, Soheil Feizi, et al. Identifying and mitigating the security risks of generative ai. *Foundations and Trends® in Privacy and Security*, 6(1):1–52, 2023. 1
- [5] Andrew Brock, Jeff Donahue, and Karen Simonyan. Large scale gan training for high fidelity natural image synthesis. *arXiv preprint arXiv:1809.11096*, 2018. 1
- [6] Baoying Chen, Jishen Zeng, Jianquan Yang, and Rui Yang. Drct: Diffusion reconstruction contrastive training towards universal detection of diffusion generated images. In *Forty-first International Conference on Machine Learning*, 2024. 2
- [7] Davide Cozzolino, Giovanni Poggi, Riccardo Corvi, Matthias Nießner, and Luisa Verdoliva. Raising the bar of ai-generated image detection with clip. In *Proceedings of the IEEE/CVF Conference on Computer Vision and Pattern Recognition*, pages 4356–4366, 2024. 2
- [8] Duc-Tien Dang-Nguyen, Cecilia Pasquini, Valentina Conotter, and Giulia Boato. Raise: A raw images dataset for digital image forensics. In *Proceedings of the 6th ACM multimedia systems conference*, pages 219–224, 2015. 5
- [9] Joel Frank, Thorsten Eisenhofer, Lea Schönherr, Asja Fischer, Dorothea Kolossa, and Thorsten Holz. Leveraging frequency analysis for deep fake image recognition. In *International conference on machine learning*, pages 3247–3258. PMLR, 2020. 2, 6, 7, 8
- [10] Fabrizio Guillaro, Davide Cozzolino, Avneesh Sud, Nicholas Dufour, and Luisa Verdoliva. Trufor: Leveraging all-round clues for trustworthy image forgery detection and localization. In *Proceedings of the IEEE/CVF conference on computer vision and pattern recognition*, pages 20606–20615, 2023. 5
- [11] Fabrizio Guillaro, Giada Zingarini, Ben Usman, Avneesh Sud, Davide Cozzolino, and Luisa Verdoliva. A bias-free training paradigm for more general ai-generated image detection. *arXiv preprint arXiv:2412.17671*, 2024. 1, 2
- [12] Yonghyun Jeong, Doyeon Kim, Youngmin Ro, Pyounggeon Kim, and Jongwon Choi. Fingerprintnet: Synthesized fingerprints for generated image detection. In *European Conference on Computer Vision*, pages 76–94. Springer, 2022. 2
- [13] Yan Ju, Shan Jia, Lipeng Ke, Hongfei Xue, Koki Nagano, and Siwei Lyu. Fusing global and local features for generalized ai-synthesized image detection. In *2022 IEEE International Conference on Image Processing (ICIP)*, pages 3465–3469. IEEE, 2022. 1, 6, 7, 8
- [14] Tero Karras, Timo Aila, Samuli Laine, and Jaakko Lehtinen. Progressive growing of gans for improved quality, stability, and variation. *arXiv preprint arXiv:1710.10196*, 2017. 2
- [15] Diederik P Kingma. Auto-encoding variational bayes. *arXiv preprint arXiv:1312.6114*, 2013. 2, 4
- [16] Bo Liu, Fan Yang, Xiuli Bi, Bin Xiao, Weisheng Li, and Xinbo Gao. Detecting generated images by real images. In *European Conference on Computer Vision*, pages 95–110. Springer, 2022. 2, 6, 7, 8
- [17] Zhengzhe Liu, Xiaojuan Qi, and Philip HS Torr. Global texture enhancement for fake face detection in the wild. In *Proceedings of the IEEE/CVF conference on computer vision and pattern recognition*, pages 8060–8069, 2020. 8
- [18] Cheng Lu, Yuhao Zhou, Fan Bao, Jianfei Chen, Chongxuan Li, and Jun Zhu. Dpm-solver: A fast ode solver for diffusion probabilistic model sampling in around 10 steps. *Advances in Neural Information Processing Systems*, 35:5775–5787, 2022. 1
- [19] Jan Lukas, Jessica Fridrich, and Miroslav Goljan. Digital camera identification from sensor pattern noise. *IEEE Transactions on Information Forensics and Security*, 1(2): 205–214, 2006. 2
- [20] Scott McCloskey and Michael Albright. Detecting gan-generated imagery using color cues. *arXiv preprint arXiv:1812.08247*, 2018. 2
- [21] Scott McCloskey and Michael Albright. Detecting gan-generated imagery using saturation cues. In *2019 IEEE international conference on image processing (ICIP)*, pages 4584–4588. IEEE, 2019. 2
- [22] Lakshmanan Nataraj, Tajuddin Manhar Mohammed, Shivkumar Chandrasekaran, Arjuna Flenner, Jawadul H Bappy, Amit K Roy-Chowdhury, and BS Manjunath. Detecting gan generated fake images using co-occurrence matrices. *arXiv preprint arXiv:1903.06836*, 2019. 2
- [23] James F O’Brien and Hany Farid. Exposing photo manipulation with inconsistent reflections. *ACM Trans. Graph.*, 31(1):4–1, 2012. 2
- [24] Utkarsh Ojha, Yuheng Li, and Yong Jae Lee. Towards universal fake image detectors that generalize across generative models. In *Proceedings of the IEEE/CVF Conference on Computer Vision and Pattern Recognition*, pages 24480–24489, 2023. 1, 2, 6, 7, 8
- [25] William Peebles and Saining Xie. Scalable diffusion models with transformers. In *Proceedings of the IEEE/CVF international conference on computer vision*, pages 4195–4205, 2023. 1
- [26] Alec Radford, Jong Wook Kim, Chris Hallacy, Aditya Ramesh, Gabriel Goh, Sandhini Agarwal, Girish Sastry, Amanda Askell, Pamela Mishkin, Jack Clark, et al. Learning transferable visual models from natural language supervision. In *International conference on machine learning*, pages 8748–8763. Pmlr, 2021. 1

- [27] Anirudh Sundara Rajan, Utkarsh Ojha, Jedidiah Schloesser, and Yong Jae Lee. On the effectiveness of dataset alignment for fake image detection. *arXiv preprint arXiv:2410.11835*, 2024. 1, 2
- [28] Jonas Ricker, Denis Lukovnikov, and Asja Fischer. Aeroblade: Training-free detection of latent diffusion images using autoencoder reconstruction error. In *Proceedings of the IEEE/CVF Conference on Computer Vision and Pattern Recognition*, pages 9130–9140, 2024. 2
- [29] Robin Rombach, Andreas Blattmann, Dominik Lorenz, Patrick Esser, and Björn Ommer. High-resolution image synthesis with latent diffusion models. In *Proceedings of the IEEE/CVF conference on computer vision and pattern recognition*, pages 10684–10695, 2022. 1, 2, 5
- [30] Robin Rombach, Andreas Blattmann, Dominik Lorenz, Patrick Esser, and Björn Ommer. Stable Diffusion. <https://github.com/Stability-AI/stablediffusion>, 2022. 2
- [31] Jiaming Song, Chenlin Meng, and Stefano Ermon. Denoising diffusion implicit models. *arXiv preprint arXiv:2010.02502*, 2020. 2, 3
- [32] Jiaming Song, Chenlin Meng, and Stefano Ermon. Denoising diffusion implicit models. *arXiv preprint arXiv:2010.02502*, 2020. 2, 3
- [33] Chuangchuang Tan, Yao Zhao, Shikui Wei, Guanghua Gu, and Yunchao Wei. Learning on gradients: Generalized artifacts representation for gan-generated images detection. In *Proceedings of the IEEE/CVF Conference on Computer Vision and Pattern Recognition*, pages 12105–12114, 2023. 1, 2, 6, 7, 8
- [34] Chuangchuang Tan, Yao Zhao, Shikui Wei, Guanghua Gu, Ping Liu, and Yunchao Wei. Rethinking the up-sampling operations in cnn-based generative network for generalizable deepfake detection. In *Proceedings of the IEEE/CVF Conference on Computer Vision and Pattern Recognition*, pages 28130–28139, 2024. 1, 6, 7, 8
- [35] Sheng-Yu Wang, Oliver Wang, Richard Zhang, Andrew Owens, and Alexei A Efros. Cnn-generated images are surprisingly easy to spot... for now. In *Proceedings of the IEEE/CVF conference on computer vision and pattern recognition*, pages 8695–8704, 2020. 2, 5, 6, 7, 8
- [36] Zhendong Wang, Jianmin Bao, Wengang Zhou, Weilun Wang, Hezhen Hu, Hong Chen, and Houqiang Li. Dire for diffusion-generated image detection. In *Proceedings of the IEEE/CVF International Conference on Computer Vision*, pages 22445–22455, 2023. 1, 2, 6, 7, 8
- [37] Danni Xu, Shaojing Fan, and Mohan Kankanhalli. Combating misinformation in the era of generative ai models. In *Proceedings of the 31st ACM International Conference on Multimedia*, pages 9291–9298, 2023. 1
- [38] Shilin Yan, Ouxiang Li, Jiayin Cai, Yanbin Hao, Xiaolong Jiang, Yao Hu, and Weidi Xie. A sanity check for ai-generated image detection. *arXiv preprint arXiv:2406.19435*, 2024. 1, 2, 5, 6, 7, 8
- [39] Nan Zhong, Yiran Xu, Sheng Li, Zhenxing Qian, and Xinpeng Zhang. Patchcraft: Exploring texture patch for efficient ai-generated image detection. *arXiv preprint arXiv:2311.12397*, 2023. 2
- [40] Nan Zhong, Yiran Xu, Zhenxing Qian, and Xinpeng Zhang. Rich and poor texture contrast: A simple yet effective approach for ai-generated image detection. *CoRR*, 2023. 2
- [41] Jun-Yan Zhu, Taesung Park, Phillip Isola, and Alexei A Efros. Unpaired image-to-image translation using cycle-consistent adversarial networks. In *Proceedings of the IEEE international conference on computer vision*, pages 2223–2232, 2017. 1
- [42] Mingjian Zhu, Hanting Chen, Qiangyu Yan, Xudong Huang, Guanyu Lin, Wei Li, Zhijun Tu, Hailin Hu, Jie Hu, and Yunhe Wang. Genimage: A million-scale benchmark for detecting ai-generated image. *Advances in Neural Information Processing Systems*, 36, 2024. 2, 5, 6, 7, 8